Revue des Composites et des Matériaux Avancés-Journal of Composite and Advanced Materials
Vol. 35, No. 1, February, 2025, pp. 87-95
Journal homepage: http://iieta.org/journals/rcma

Synthesis of a Gel Electrolyte Membrane Based on PVA/KCl/Glycerol Doped with CQDs for Aluminum Ion Battery Applications

Firman Ridwan*, Muhammad Akbar Husin, Nanda Febriyan

Department of Mechanical Engineering, Andalas University, Padang 25163, Indonesia

Corresponding Author Email: firmanridwan@eng.unand.ac.id

https://doi.org/10.18280/rcma.350111

Received: 29 November 2024
Revised: 16 December 2024
Accepted: 14 January 2025
Available online: 28 February 2025

Keywords:
CQD, Al-Battery, ionic conductivity, gel electrolyte, battery capacity, KCl

ABSTRACT

This study investigates the synthesis and characterization of a gel electrolyte membrane based on polyvinyl alcohol (PVA), potassium chloride (KCl), and glycerol doped with carbon quantum dots (CQDs) for aluminum-ion battery applications. This study synthesized carbon quantum dots and doped them into a PVA/KCl/glycerol gel electrolyte membrane, significantly improving the ionic conductivity, specific capacity, and cycling stability of aluminum-ion batteries. CQDs were synthesized using a microwave-assisted method with citric acid and urea as precursors. Five variations of the electrolyte membrane were prepared by incorporating different concentrations of CQDs into the PVA/KCl/glycerol mixture. Scanning electron microscope (SEM) analysis revealed that increasing the CQD concentration led to a more compact and interconnected particle structure within the electrolyte membrane. Galvanostatic discharge tests showed that the CQD0 membrane, with the highest CQD concentration, exhibited the longest discharge time of 713.9 seconds at 1mA. Electrochemical impedance spectroscopy (EIS) measurements indicated that the CQD0 membrane had the lowest impedance of 1185.25Ω and the highest ionic conductivity of 0.84mS/cm. The capacity density and power density of the CQD0 membrane were found to be 0.231713 mAh/cm^2 and 21.45 mW/cm, respectively. The results suggest that incorporating CQDs into the PVA/KCl/glycerol gel electrolyte membrane enhances the electrochemical performance and conductivity of the aluminum-ion battery. This study highlights the potential of utilizing CQD derived from organic waste materials as electrolyte additives to improve battery characteristics while mitigating adverse environmental effects.

1. INTRODUCTION

Aluminum-ion (Al-ion) batteries possess significant potential as an energy storage technology due to their low cost [1] and high energy density [1-3]. Innovation in battery technology is needed because currently conventional batteries face several challenges, such as high costs [4] and thermal issues [5-7]. Alongside the increasing demand for batteries, alternative battery technologies are also rapidly evolving. Aluminum, an abundant material in the Earth's crust with the largest reserves among metals, is a focus of this research [8]. Aluminum batteries, with several advantages, are emerging as potential replacements for conventional batteries. They offer an energy density four times higher than lithium batteries [1] and are less prone to short-circuiting [9].

Nevertheless, Al-air batteries face challenges regarding cycle stability and catalytic efficiency that need to be addressed. The anode presents certain limitations in its development; therefore, innovations are focused on the electrolyte to enhance battery performance and stability. A novel approach to enhance the efficiency and reliability of Al-air batteries involves incorporating carbon quantum dots (CQD) into the electrolyte [10]. CQDs, due to their extremely small size, exhibit remarkable electrocatalytic capabilities and conductivity, leading to improved total energy efficiency [11, 12]. Moreover, CQD may be synthesized using a wide range of organic substances that are readily available and have minimal impact on the environment. This makes CQDs a viable and economically viable choice for enhancing the durability and efficiency of Al-ion batteries.

CQDs have been demonstrated to enhance battery efficacy in numerous prior studies. Jin et al. [13] reported a high-performance CQD/hG composite catalyst for Li-CO_2 batteries, achieving a low overpotential of 1.02V, a discharge capacity of 12300 mAh/g, and excellent stability with 235 cycles, due to its high catalytic activity and fast electron/electrolyte transport. The CQD-Bi_2O_3 composite anode material in lithium-ion batteries exhibited exceptional electrochemical activity and a discharge capacity of 1500 mAh/g in a comparable investigation conducted by Prasath et al. [14]. The specific capacity of CQDs used as an anode in sodium-ion batteries was 323.9 mAh/g, and the capacity retention was 72.4% after 500 charge/discharge cycles, as indicated by a separate study conducted by Javed et al. [15]. These findings indicate that CQDs exhibit exceptional cycling stability. To enhance the performance, polyvinyl alcohol (PVA) was used

as the matrix due to its advantageous characteristics, such as excellent solubility in water, which facilitates integration and processing with fibers, as well as its elasticity and flexibility, enabling it to withstand deformation [16]. PVA possesses biocompatibility and non-toxic characteristics, rendering it environmentally friendly [17]. Aluminum batteries with PVA-based electrolytes and CQDs provide significant environmental benefits. PVA is biodegradable and reduces harmful chemicals, while CQDs, made from biomass, minimize the use of toxic materials. Aluminum itself has a lower carbon footprint than lithium-ion, and the combination of PVA and CQDs enhances sustainability through better recycling and waste reduction, leading to an overall decrease in environmental impact.

Prior studies have demonstrated that CQDs enhance the electrical characteristics of anodes and cathodes in metal ion batteries, hence improving features such as conductivity, capacity, and stability. Interestingly, there has been no research conducted on the use of CQDs in Al-ion batteries. The objective of this investigation is to ascertain the most effective concentration for conductivity when using CQDs as a raw material in gel electrolytes. A PVA/KCl/Glycerol polymer electrolyte membrane was combined with five variations of CQDs that were synthesized using a microwave-assisted method. These variations differ based on the composition of CQD particles in the electrolyte. The study endeavors to improve battery performance by modifying the composition of CQD particles, which will improve membrane characteristics, ion transport, and conductivity. Furthermore, the utilization of organic waste materials as electrolyte additives through CQD particles can assist in the mitigation of adverse environmental effects.

2. MATERIAL AND METHOD

2.1 Material

To produce Carbon Quantum Dots (CQD), citric acid and urea obtained from Merck. The battery electrolyte is prepared using main ingredients namely PVA (Polyvinyl Alcohol), KCl (Potassium Chloride), and glycerol, also sourced from Merck. These materials are chosen for their high purity and consistency in delivering optimal results. Additionally, distilled water and 70% alcohol are sourced from a local store.

2.2 Preparation of CQD

Figure 1. Photograph of CQD0, CQD10, CQD20, CQD30 and CQD40 when illuminated under UV light of 405 nm wavelength

The process of making CQD adopts the method described in the journal by Kumar et al. [18]. 3 g of citric acid and 3 g of urea were added as precursors to 10 ml of distilled water and stirred until the solution became homogeneous. The solution was then heated in a 700-watt microwave on high for 2 minutes until it dried, changing from a transparent liquid to a dark brown solid. The solid was then added to 10 ml of distilled water and microwaved for 3 minutes, repeating the process twice. Afterward, a black solid was obtained, which was added to 50 ml of water and sonicated for 30 minutes until it dissolved, resulting in a CQD solution. The CQD solution was partitioned into five 10 ml samples. The initial sample received an addition of 40 ml of distilled water (CQD40), succeeded by 30, 20, 10, and 0 ml of distilled water for CQD30, CQD20, CQD10, and CQD0, respectively, as shown in Figure 1.

2.3 Fabrication of electrolyte membrane

The solid electrolyte membrane was made through several steps. The electrolyte preparation began by dissolving 4g of PVA in 100 ml of distilled water at 80℃ while stirring at 600rpm for 30 minutes. Once the PVA solution was homogeneous, 1.5 g of KCl was added and stirred for 30 minutes until the mixture was well combined. Then, 0.4 ml of glycerol was added and stirred for another 30 minutes. Next, 2 ml CQD0 was added to the solution and stirred at 60℃ for one hour until the solution thickened. The same procedure was repeated for CQD10, CQD20, CQD30, and CQD40. Finally, the solution was poured into battery and tensile testing molds, and then left at room temperature for 24 hours. The assembled battery is illustrated in Figure 2.

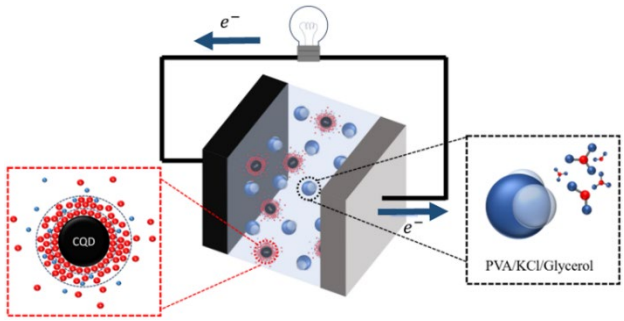

Figure 2. Fabrication of gel electrolyte membrane

3. RESULTS AND DISCUSSION

3.1 Scanning electron microscope analysis (SEM)

The SEM analysis in Figure 3 reveals the relationship between the morphological structure of the PVA/KCl/Glycerol/CQD composite and variations in CQD concentration. In Figure 3, PVA granules appear as the primary matrix phase with a rough and predominantly amorphous morphology, exhibiting a layered texture and uneven surface that form the composite foundation, providing the necessary flexibility and mechanical properties. Glycerol acts as a plasticizer that enhances the flexibility and homogeneity of the PVA matrix by filling the gaps between the granules, thereby strengthening the interaction between PVA and the filler material, namely CQD. Increasing the CQD concentration in the PVA/KCl/Glycerol composite affects

material density, particle distribution, and surface morphology, where higher CQD concentrations result in more uniform distribution, increased density, and a more homogeneous surface morphology. With glycerol serving as a flexible binder in the matrix and PVA acting as the backbone of the composite, optimizing the CQD concentration is crucial to achieving the best mechanical properties and morphology.

Figure 3 illustrates the electrolyte membrane as examined using an electron microscope. The initial image, denoted as Figure 3(a), exhibits the most elevated concentration of CQD, with notably compact interconnections among the particles. Continuing with Figure 3(b), there is a small reduction in density. Figure 3(c) shows a decrease in the number of CQD particles, which indicates sparse between particles. According to Figure 3(d), it seems that the concentration of CQD decreases throughout the membrane. Figure 3 (e) clearly demonstrates a substantial reduction in interaction within the PVA/KCl/Glycerol mixture. The interaction between CQD and the PVA/KCl/Glycerol mixture results in the creation of a composite solid electrolyte with a surface structure that enhances the density between particles. Greater dispersion leads to higher ionic conductivity in electrolytes [19].

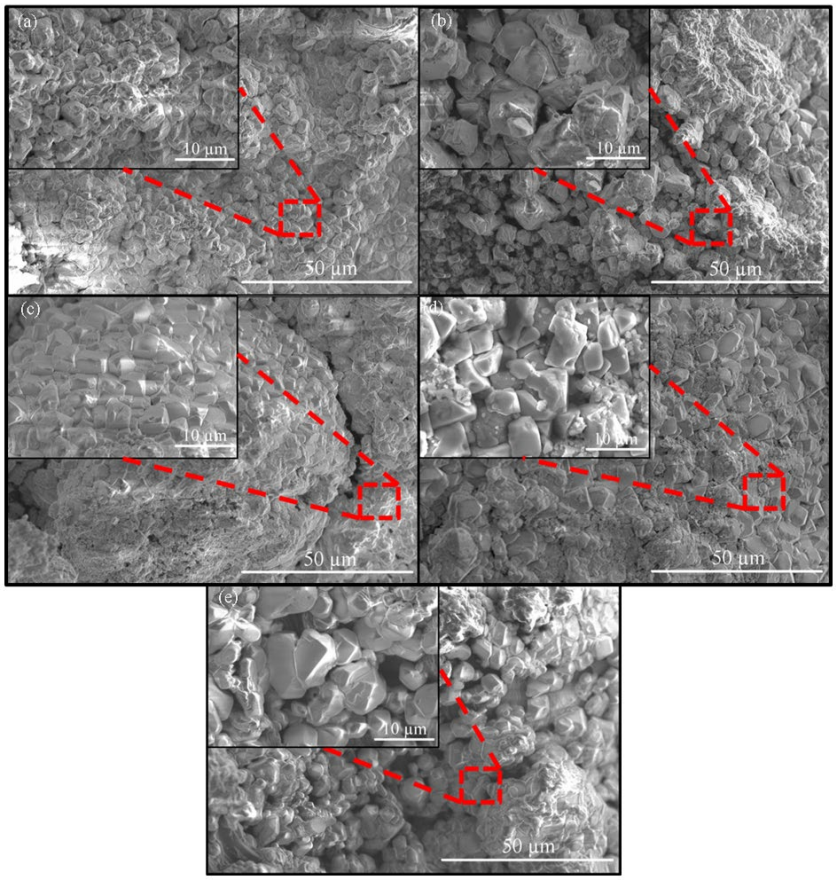

Figure 3. SEM morphology of PVA/KCl/Glycerol electrolyte membrane with the addition of (a) CQD0, (b) CQD10, (c) CQD20, (d) CQD30, (e) CQD40

3.2 FTIR spectroscopic evaluation

Figure 4 shows the FTIR spectrum of several electrolyte membrane samples with varying CQD additions, namely CQD40, CQD30, CQD20, CQD10, and CQD0. The x-axis represents the wavelength (cm^{-1}), indicating the infrared absorption frequency, while the y-axis represents the transmittance (T%), which shows the amount of infrared light transmitted through the sample.

The FTIR graph shown in Figure 4 (a) presents the infrared spectrum of each sample, with specific regions highlighted for more detailed analysis. Figure 4 (b) illustrates the wavelength area of 3625 cm^{-1}, corresponding to O-H stretching, signifying the presence of carboxylic acid groups [20]. Permatasari et al. [21] indicate that the majority of cases involving CQDs are significantly associated with surface passivation via functionalization or modification. The predominant surface functionalization entails oxygen-containing functional groups (e.g., carbonyl, carboxyl) and nitrogen-containing functional groups (e.g., amine).

The absorption intensity in this region varies between samples, with CQD40 showing the lowest absorption, suggesting fewer OH groups compared to the other samples. Figure 4 (c) similarly exhibits absorption bands about 2830 cm^{-1}, associated with C-H stretching, predominantly from aliphatic molecules [20]. Although the absorption in this region is relatively low, it still varies among samples, reflecting differences in hydrocarbon content. Furthermore, in Figure 4 (d), significant absorption is observed at 1645 cm^{-1}, which can be attributed to C=C stretching vibrations, indicating the presence of carbon-carbon double bonds commonly found in aromatic or alkene structures [20]. The varying absorption intensities across different regions for each sample indicate distinct differences in their chemical compositions, particularly in the presence of O-H, C-H, and C=C groups. These variations in absorption intensity and peak positions suggest that each sample contains differing amounts of functional groups, which may influence the material's physical and chemical properties.

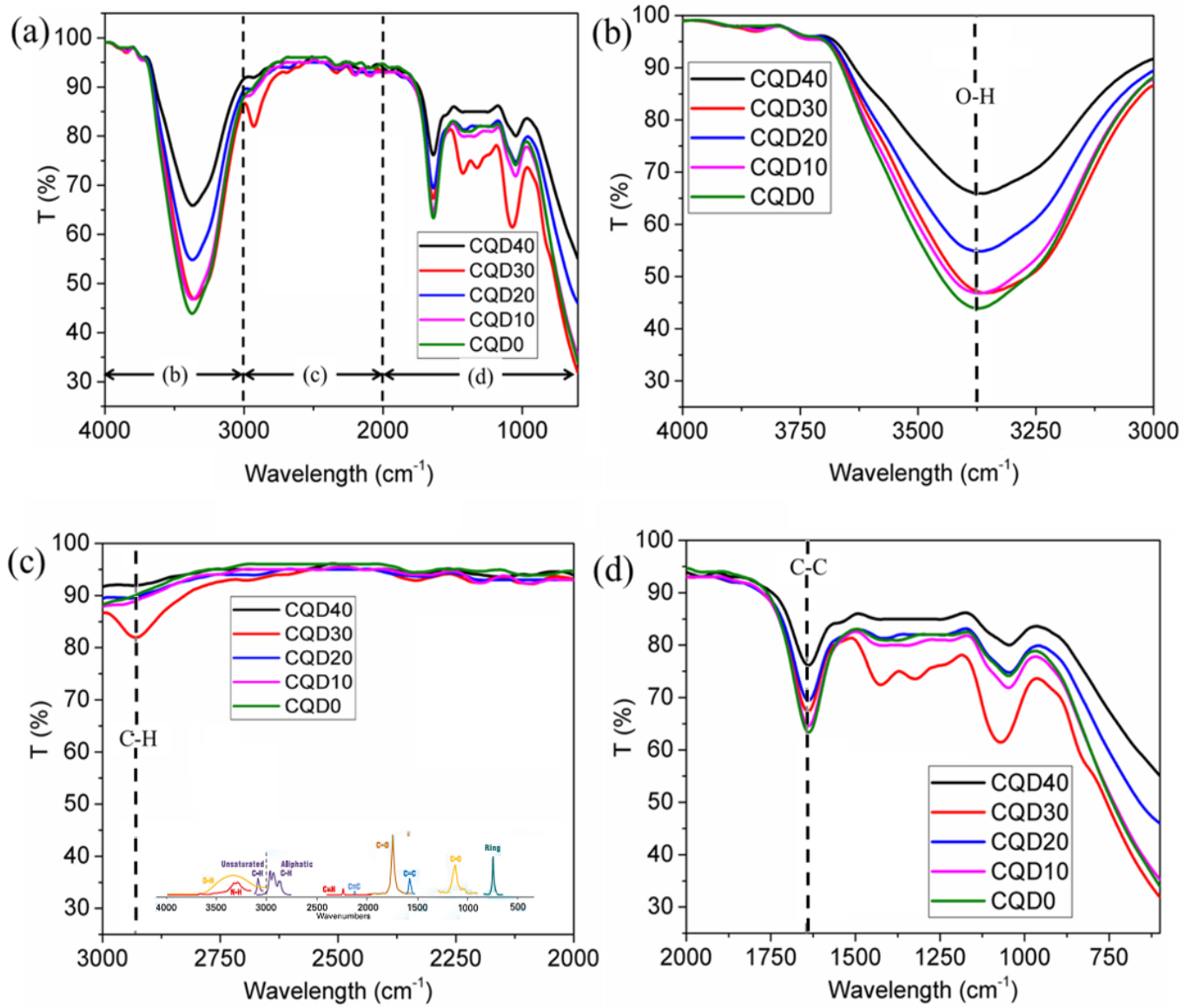

Figure 4. FTIR spectrum of PVA/KCl/Glycerol electrolyte membrane with variations in CQD addition at wavelengths (a) 4000-600cm^{-1}, (b) 4000-3000cm^{-1}, (c) 3000-2000cm^{-1} and (d) 2000-600cm^{-1}

3.3 X-rays crystallographic examination

X-Ray Diffraction (XRD) testing is an analytical technique used to determine the crystal structure and composition of materials. Figure 5 shows a diffraction pattern with several sharp peaks, indicating a high degree of crystallinity in the PVA/KCl/Glycerol/CQD0 electrolyte membrane. The highest intensity peak is observed at a 2θ angle between 35° and 40°. Crystallinity peaks occur at 2θ angles of 28.5°, 40.6°, 44.5°, 50.3°, 58.7°, 66.5°, 73.8°, 81.4°, 87.8°, and 94.6°, indicating the presence of multiple crystal planes in the material's structure. The sharp peaks suggest large, well-ordered crystals, while the distribution of peaks points to the possible existence of more than one crystal phase. Based on the crystallinity peak data, the average crystal size of the PVA/KCl/Glycerol/CQD0 membrane is approximately 50.6nm. Based on Figure 5, it can be observed that the peak degree of crystallinity for PVA is at 40.6°, which aligns with findings from Aziz et al. [22], indicating a crystallinity angle of 41.6° for PVA. Meanwhile, the peak crystallinity of CQD is recorded at 28.5°, consistent with previous research showing the crystallinity peak of carbon dots at 28.4° [23].

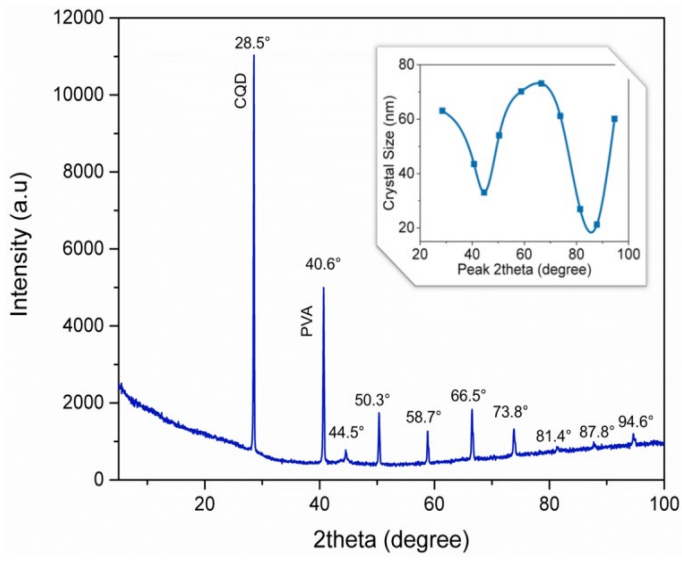

Figure 5. XRD graph of PVA/KCl/Glycerol/CQD0 electrolyte membrane

3.4 XRF elemental analysis

The chemical composition of aluminum alloy as anode is ascertained via X-ray fluorescence (XRF) to identify the elemental components and their respective concentrations. Figure 6 illustrates the percentage composition of elements present in aluminium alloys. The aluminium content consists mainly of Aluminium (Al, 97.58%), with notable impurities including Copper (Cu, 0.224%), Iron (Fe, 0.726%), Silicon (Si, 0.63%), and other trace elements. Furthermore, there are additional minerals, such as manganese (Mn, 0.0051%) and titanium (Ti, 0.047%).

Aluminum, being the main active material, plays a critical role in the performance of the battery due to its high theoretical capacity. The presence of trace elements, such as iron and silicon, could originate from impurities in the raw material or the manufacturing process. These impurities may influence the anodic reaction by increasing self-corrosion rates or forming passive oxide layers that hinder electron flow, thereby reducing battery efficiency.

Understanding the composition and purity of the anode material is essential, as it directly impacts the battery's discharge performance, energy output, and overall efficiency. Optimizing the chemical composition of the anode can reduce unwanted side reactions, improve electron discharge processes, and extend battery life.

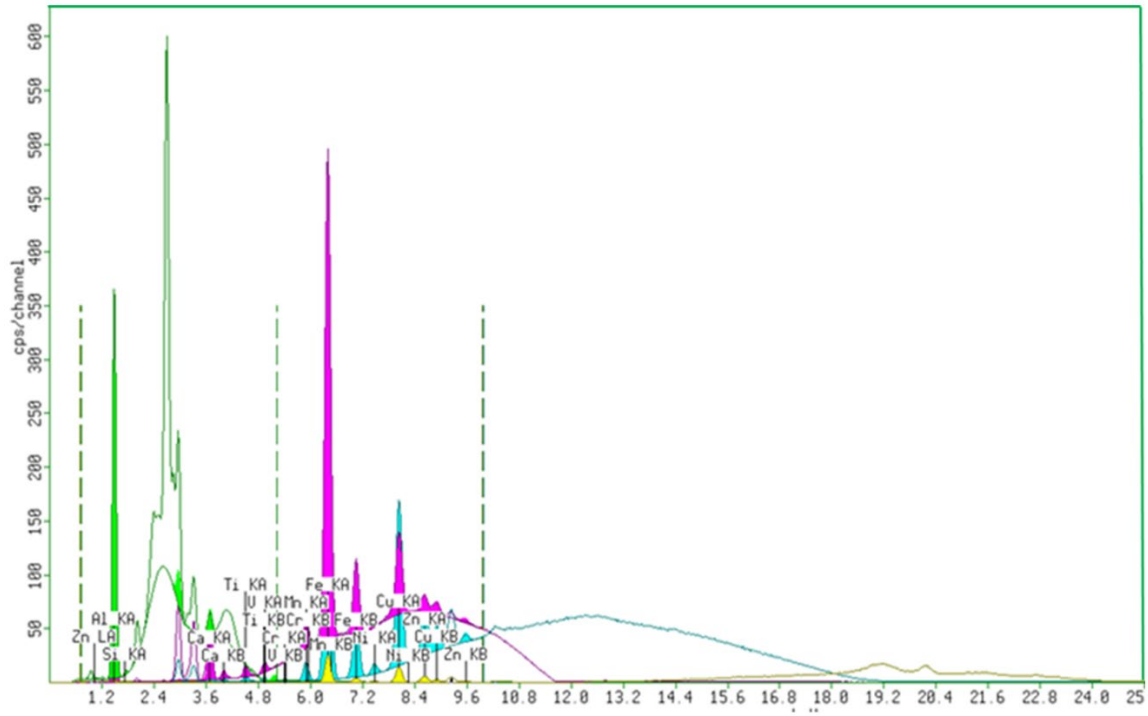

Figure 6. XRF graph of aluminium anode

3.5 Discharging

Galvanostatic discharge is a method in electrochemistry in which a constant electric current is applied to a cell or battery during the discharge process [24]. In the context of a battery, this means a constant current is applied until the battery is fully discharged, and the cell voltage is measured as a function of time. This process is used to characterize the performance and capacity of the battery. The results of galvanostatic discharge testing are presented in the form of a voltage versus time graph, as shown in Figure 7.

Figure 7 shows galvanostatic discharging test, the CQD0 sample exhibited the highest durability, lasting for 713.9 seconds at a current of 1 mA with an initial voltage of 1.35 V. In contrast, CQD10 had a discharge time of 690.5 seconds with an initial voltage of 1.28 V, slightly lower than CQD0. CQD0 contains a higher concentration of CQD due to the denser distribution of carbon nanoparticles in the electrolyte solution. Surface functional groups, which are groups of atoms that are bound to the surface of solid objects, such as carbon, diamond, graphite, or silicon dioxide, are present in CQDs, as previously mentioned. The absorption characteristics and porous properties of the material are influenced by surface functional groups. Ion exchange is enabled by this absorption mechanism [25].

When the CQD content was reduced to CQD20, the discharge duration drastically decreased to 459.8 seconds, despite a slightly higher initial voltage of 1.3 V. Further performance decline was observed with CQD30, which lasted 335.7 seconds with an initial voltage of 1.21 V. Finally, CQD40 exhibited the lowest durability, lasting only 305.2 seconds at the same current, with an initial voltage of 1.27 V. The addition of CQD in the battery membrane can enhance capacity and long cycle life [26]. With the presence of CQD, the charge transfer pathways become more efficient, enabling electrochemical reactions to occur more rapidly and optimally, contributing to an increase in energy storage capacity.

The incorporation of CQD in batteries can improve the interface between the electrolyte and the electrode, so expediting the redox (reduction-oxidation) reactions and augmenting the charging and discharging rates. An increased quantity of CQD in the system results in a greater active surface area on the electrode, hence offering more opportunities for interaction with electrolyte ions. This facilitates more effective electron transmission, accelerates the chemical reactions within the battery, and enhances its capacity.

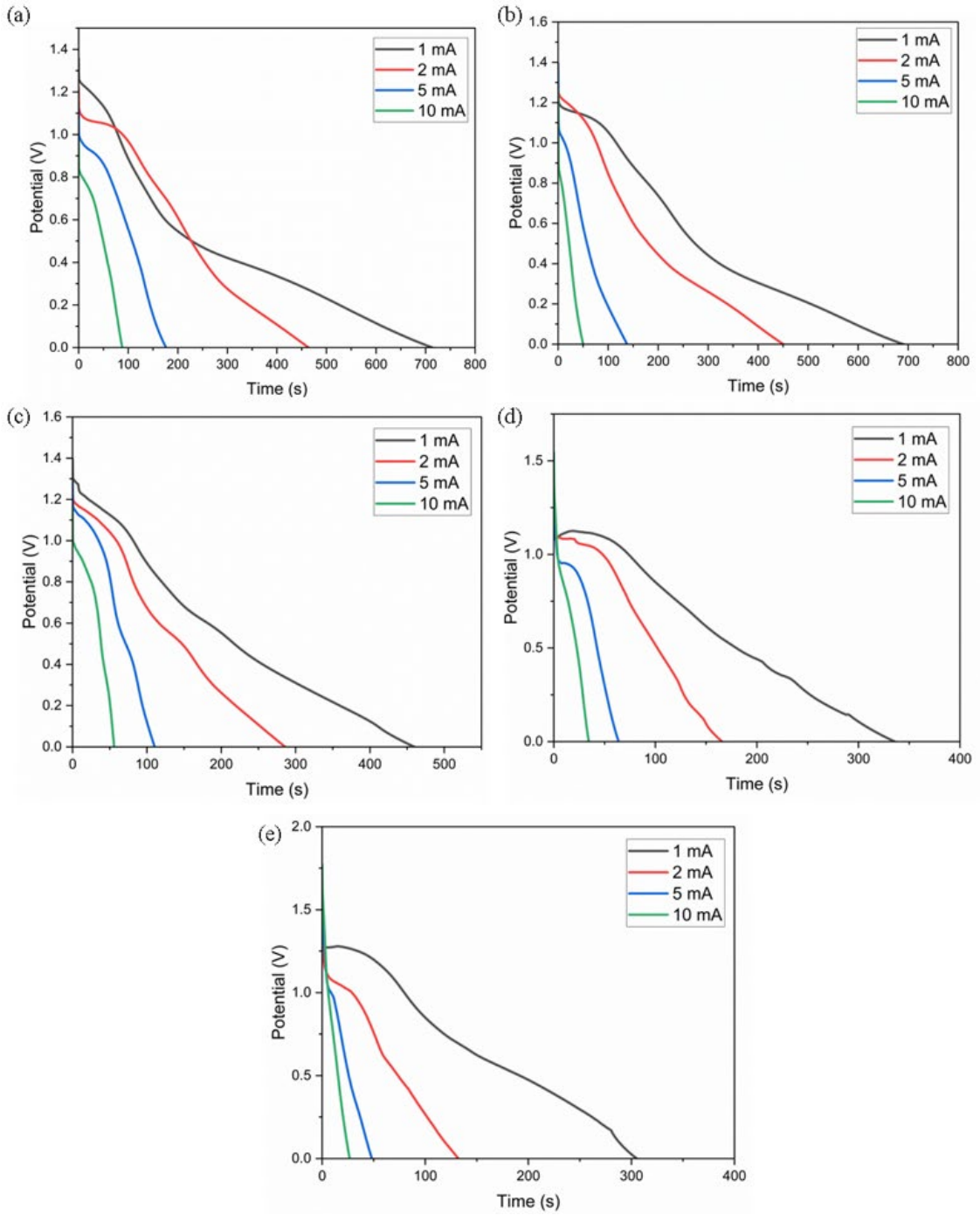

Figure 7. Galvanostatic discharging of Al-air battery using electrolyte PVA/KCl/Glycerol (a) CQD0, (b) CQD10, (c) CQD20, (d) CQD30, (e) CQD40

Table 1 demonstrates that with increasing CQD content, both capacity and capacity density improve. CQD0, with the highest CQD concentration, shows the greatest capacity at 0.926852mAh and a capacity density of 0.231713 mAh/cm². As the CQD content decreases, such as in CQD10 and CQD20, both capacity and capacity density gradually decline. The lowest values are observed in CQD40, which has no added CQD, with a capacity of 0.339111 mAh and a capacity density of 0.084778 mAh/cm². This trend indicates that higher CQD content leads to enhanced energy storage performance. The increase in capacity and capacity density with more CQD is due to CQDs' conductivity which enhance charge transfer and create more active sites for energy storage [27]. This leads to improved electrochemical efficiency and better overall battery performance as CQD content increases.

Table 1. Capacity and capacity density of battery samples

Sample	Capacity (mAh)	Capacity Density (mAh/cm^2)
CQD0	0.926852	0.231713
CQD10	0.767333	0.191833
CQD20	0.511000	0.127750
CQD30	0.373074	0.093269
CQD40	0.339111	0.084778

3.6 Electrical properties evaluation

Electrochemical Impedance Spectroscopy (EIS) is an analytical method used to assess the impedance response of electrochemical systems, such as batteries, to tiny alternating current (AC) disturbances in order to model the movement of

ions. Electrochemical impedance spectroscopy (EIS) is conducted under potentiostatic conditions, with a frequency range spanning from 10 mHz to 100 kHz. At low measurement frequencies, battery diffusion behavior is commonly represented by the Warburg impedance [28]. As real impedance increases, the resulting frequency declines [29]. The applied voltage comprises a 10mV root mean square (mVrms) alternating current (AC). Impedance graphs depict in Figure 8 the primary impedance components, which are resistance (Z_{re}) and reactance (Z_{im}). Zre represents the electrical resistance that hinders electric current movement, while Z_{im} represents the reactance influenced by energy storage components like inductors and capacitors. Impedance analysis is a useful tool for comprehending battery performance within the realm of batteries. Z_{re} provides insights into the impact of internal resistance on energy efficiency and conductivity, whereas Z_{im} describes energy storage and release properties, as well as conditions that lead to battery degradation.

In Figure 8, it can be observed that the battery membrane with the lowest concentration of CQDs (CQD40) exhibits the highest resultant impedance of 3630.42 Ω. The impedance values decrease sequentially with increasing CQD concentration; CQD30, CQD20, CQD10, and CQD0 each have impedance values of 2474.14, 2081.58, 1998.10 and 1185.25 Ω.

Impedance is a measure of the total resistance encountered by an electric current flowing through an electrical circuit, indicating that higher impedance of the electrolyte membrane correlates with lower conductivity. Table 2 shows increased conductivity with rising CQD concentration, with the highest conductivity observed in the mixed CQD0 membrane at 0.84 mS/cm. Previous Al-battery research using PVA/KOH/Glycerol/NCC Nanofiber electrolyte only produced an ionic conductivity of 0.068 mS/cm [30]. The distribution of CQD particles in the electrolyte membrane is responsible for the increase in conductivity, as they occupy the empty space gaps in the membrane [10].

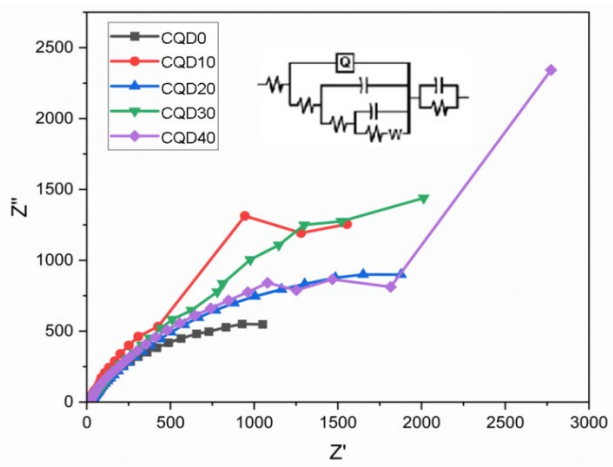

Figure 8. EIS plot of various CQD electrolyte

Table 2. Ionic conductivity of battery samples

Sample	Ionic Conductivity (mS/cm)
CQD0	0.84
CQD10	0.5
CQD20	0.48
CQD30	0.4
CQD40	0.27

3.7 Electrochemical behavior assessment

Figure 9 depicts the intensity of the reduction and oxidation reaction peaks as well as the kinetics of the electrochemical reactions under varying voltage conditions, both upward and downward. CQD0 shows a significant increase in power and exhibits a heightened intensity of electrochemical processes, leading to more pronounced reduction and oxidation reactions.

Based on Figure 9, the cyclic voltammetry (CV) test findings indicate a variation in the oxidation and reduction peak currents as the concentration of CQD diminishes. For CQD0, exhibiting the highest concentration, the oxidation peak attains 0.0145 A/cm², whereas the reduction peak approximates -0.0025 A/cm², signifying a rapid electrochemical response. For CQD10, the oxidation peak current marginally diminishes to 0.0130A/cm², accompanied by a modest fall in the reduction peak, signifying a decline in reaction efficiency. Additional reductions are noted for CQD20 and CQD30, exhibiting oxidation peak currents of 0.0120 A/cm² and 0.0110 A/cm², signifying a reduced oxidation reaction rate. In CQD40, the lowest concentration exhibits a singular substantial oxidation peak at 0.0045 A/cm², suggesting suppression of the electrochemical reaction, potentially attributable to structural alterations or other variables influencing reaction kinetics. The result demonstrates a reduction in electrochemical reaction rates as CQD concentration diminishes, signifying alterations in reaction kinetics.

Table 3 demonstrates that increasing the amount of CQD leads to higher power and power density of the battery [14]. CQD0, which contains the highest concentration of CQD, exhibits the greatest power density at 21.45 mW/cm² and a power output of 85.80 mW. In contrast, as the CQD content decreases, both power density and power also decline, with CQD10 showing a power density of 18.75 mW/cm² and a power of 75.00 mW, followed by CQD20 at 11.55 mW/cm² and 46.20mW. The trend continues with CQD30 and CQD40, where power density drops to 10.35 mW/cm² and 4.80 mW, respectively, indicating that the addition of CQD significantly enhances the battery's performance.

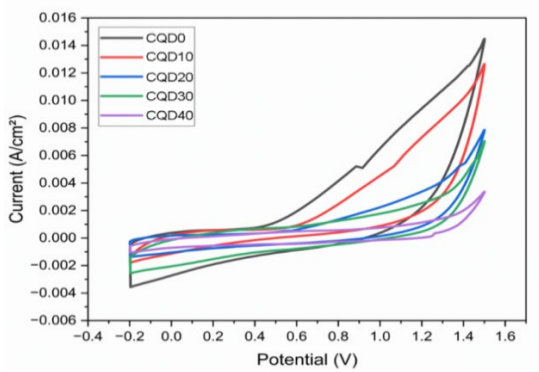

Figure 9. Cyclic voltammetry of various electrolyte membrane

Table 3. Power and power density of battery samples

Sample	Power Density (mW/cm²)	Power (mW)
CQD0	21.45	85.80
CQD10	18.75	75.00
CQD20	11.55	46.20
CQD30	10.35	41.40
CQD40	4.80	19.20

In addition to the incorporation of CQD into gel electrolyte membranes, there are several other promising strategies for enhancing the performance of aluminum-ion batteries. One potential approach is optimizing the electrode materials, as the efficiency of the electrochemical reactions in the battery largely depends on the properties of the anode and cathode. The use of advanced materials, such as graphene-based electrodes or carbon nanotubes, could significantly improve the battery's energy density and charge/discharge rates. Another strategy involves modifying the electrolyte composition to enhance ionic conductivity and stability. This could include the use of novel solid-state electrolytes or ionic liquids that offer improved performance in terms of both safety and efficiency. Additionally, incorporating conductive additives into the electrolyte or electrode materials may help reduce internal resistance, further enhancing battery performance. Future research should explore the synergistic effects of combining these strategies with the CQD-modified electrolytes to achieve the optimal performance in aluminium-ion batteries.

4. CONCLUSION

This study explores the innovative use of CQD in gel electrolyte membranes for aluminum-air batteries, a promising strategy to enhance battery performance. By synthesizing CQDs using citric acid and urea and incorporating them into a PVA/KCl/Glycerol polymer electrolyte membrane, this research demonstrates that higher CQD concentrations improve the discharge time, capacity, and ionic conductivity of the battery. SEM analysis revealed that higher CQD concentrations resulted in more compact particle interconnections. Galvanostatic discharge testing showed that the battery with the highest CQD concentration (CQD0) had the longest discharge time of 713.9 seconds at 1mA and highest capacity of 0.92 mAh. Electrochemical impedance spectroscopy (EIS) demonstrated that increasing CQD concentration led to lower impedance and higher ionic conductivity, with CQD0 exhibiting the highest conductivity of 0.84 mS/cm. The study aims to improve battery performance by modifying the composition of CQD particles in the electrolyte membrane.

FUNDING

This research is financed by the Directorate General of Higher Education, Research, and Technology Ministry of Education, Culture, Research, and Technology of Indonesia by the research contract number 041/E5/ PG.02.00.PL/2024.

AUTHOR CONTRIBUTIONS

Firman Ridwan: Conceptualization, Methodology, Validation, and Supervision, Data Curation, Investigation, and Writing original draft. Muhammad Akbar Husin: Visualization, Software and SEM Analysis. Nanda Febriyan : Sample Preparation.

REFERENCES

[1] Leisegang, T., Meutzner, F., Zschornak, M., Münchgesang, W., Schmid, R., Nestler, T., Eremin, R.A., Kabanov, A.A., Blatov, V.A., Meyer, D.C. (2019). The aluminum-Ion battery: A sustainable and seminal concept?. Frontiers in Chemistry, 7: 268. https://doi.org/10.3389/fchem.2019.00268

[2] Farsak, M., Kardaş, G. (2018). 2.12 Electrolytic materials. Comprehensive Energy Systems, 2: 329-367. https://doi.org/10.1016/B978-0-12-809597-3.00225-X

[3] Wen, X., Guo, J. (2022). Aluminum ion batteries. Encyclopedia of Energy Storage, 4: 223-230. https://doi.org/10.1016/B978-0-12-819723-3.00018-4

[4] Yang, H., Li, H., Li, J., Sun, Z., He, K., Cheng, H.M., Li, F. (2019). The rechargeable aluminum battery: Opportunities and challenges. Angewandte Chemie International Edition, 58(35): 11978-11996. https://doi.org/10.1002/anie.201814031

[5] Cao, R., Zhang, X., Yang, H. (2023). Prediction of the heat generation rate of lithium-Ion batteries based on three machine learning algorithms. Batteries, 9(3): 165. https://doi.org/10.3390/batteries9030165

[6] Cao, R., Zhang, X., Yang, H., Wang, C. (2023). Experimental study on heat generation characteristics of lithium-Ion batteries using a forced convection calorimetry method. Applied Thermal Engineering, 219: 119559. https://doi.org/10.1016/j.applthermaleng.2022.119559

[7] Kannan, C., Vignesh, R., Karthick, C., Ashok, B. (2021). Critical review towards thermal management systems of lithium-ion batteries in electric vehicle with its electronic control unit and assessment tools. Proceedings of the Institution of Mechanical Engineers, Part D: Journal of Automobile Engineering, 235(7): 1783-1807. https://doi.org/10.1177/0954407020982865

[8] Asmare, M., Zegeye, M., Ketema, A. (2024). Advancement of electrically rechargeable metal-Air batteries for future mobility. Energy Reports, 11: 1199-1211. https://doi.org/10.1016/j.egyr.2023.12.067

[9] Yang, S., Wang, W., Lin, C., Shen, W., Li, Y. (2019). Investigation of internal short circuits of lithium-Ion batteries under mechanical abusive conditions. Energies, 12(10): 1885. https://doi.org/10.3390/en12101885

[10] Ma, C., Dai, K., Hou, H., Ji, X., Chen, L., Ivey, D.G., Wei, W. (2018). High ion-Conducting solid-State composite electrolytes with carbon quantum dot nanofillers. Advanced Science, 5(5): 1700996. https://doi.org/10.1002/advs.201700996

[11] Hu, Y., Chen, W., Lei, T., Zhou, B., Jiao, Y., Yan, Y., Du, X., Huang, J., Wu, C., Wang, X., Wang, Y., Chen, B., Xu, J., Wang, C., Xiong, J. (2019). Carbon quantum dots-Modified interfacial interactions and ion conductivity for enhanced high current density performance in lithium-Sulfur batteries. Advanced Energy Materials, 9(7): 1802955. https://doi.org/10.1002/aenm.201802955

[12] Tian, L., Li, Z., Wang, P., Zhai, X., Wang, X., Li, T. (2021). Carbon quantum dots for advanced electrocatalysis. Journal of Energy Chemistry, 55: 279-294. https://doi.org/10.1016/j.jechem.2020.06.057

[13] Jin, Y., Hu, C., Dai, Q., Xiao, Y., Lin, Y., Connell, J. W., Chen, F., Dai, L. (2018). High-Performance Li-CO2 batteries based on metal-Free carbon quantum dot/holey graphene composite catalysts. Advanced Functional Materials, 28(47): 1804630. https://doi.org/10.1002/adfm.201804630

[14] Prasath, A., Athika, M., Duraisamy, E., Selva Sharma,

A., Sankar Devi, V., Elumalai, P. (2019). Carbon quantum dot-anchored bismuth oxide composites as potential electrode for lithium-Ion battery and supercapacitor applications. ACS Omega, 4(3): 4943-4954. https://doi.org/10.1021/acsomega.8b03490

[15] Javed, M., Saqib, A.N.S., Ali, B., Faizan, M., Anang, D.A., Iqbal, Z., Abbas, S.M. (2019). Carbon quantum dots from glucose oxidation as a highly competent anode material for lithium and sodium-Ion batteries. Electrochimica Acta, 297: 250-257. https://doi.org/10.1016/j.electacta.2018.11.167

[16] Mohammed, K.A., Shihab, S.A.A., Algburi, S., Bhavani, B., Ali, K., Alkhafaji, M.A., Rahman, Z., Sharma, S. (2024). Synthesis and characterization of PVA-encapsulated Fe2O3-ZnO as new composites with tunable optical properties. Revue des Composites et des Matériaux Avancés, 34(2): 163-167. https://doi.org/10.18280/rcma.340205

[17] Kadhim, I.A.U., Taeh, A.S., Abed, M.S. (2024). Sodium alginate substrate coated with PVA/Nanosilver composite nanofibers for skin tissue engineering. Revue des Composites et des Materiaux Avances, 34(3): 305-313. https://doi.org/10.18280/rcma.340305

[18] Kumar, P., Bhatt, G., Kaur, R., Dua, S., Kapoor, A. (2020). Synthesis and modulation of the optical properties of carbon quantum dots using microwave radiation. Fullerenes, Nanotubes and Carbon Nanostructures, 28(9): 724-731. https://doi.org/10.1080/1536383X.2020.1752679

[19] Ridwan, F., Agusta, D., Husin, M.A., Dahlan, D. (2025). Evaluation of the addition of cement ash to the PVA/TEOS/HCl gel electrolyte on the performance of aluminium air batteries. Materials Science for Energy Technologies, 8: 24-31. https://doi.org/10.1016/j.mset.2024.07.003

[20] Sigma-Aldrich. (2019). IR Spectrum Table & Chart. https://www.scribd.com/document/432355477/IR-Spectrum-Table-Chart-Sigma-Aldrich.

[21] Permatasari, F.A., Irham, M.A., Bisri, S.Z., Iskandar, F. (2021). Carbon-based quantum dots for supercapacitors: Recent advances and future challenges. Nanomaterials, 11(1): 91. https://doi.org/10.3390/nano11010091

[22] Aziz, S.B., Brza, M.A., Dannoun, E.M., Hamsan, M.H., Hadi, J.M., Kadir, M.F., Abdulwahid, R.T. (2020). The study of electrical and electrochemical properties of magnesium ion conducting CS: PVA based polymer blend electrolytes: Role of lattice energy of magnesium salts on EDLC performance. Molecules, 25(19): 4503. https://doi.org/10.3390/molecules25194503

[23] Sharma, N., Sharma, I., Bera, M.K. (2022). Microwave-assisted green synthesis of carbon quantum dots derived from calotropis gigantea as a fluorescent probe for bioimaging. Journal of Fluorescence, 32(3): 1039-1049. https://doi.org/10.1007/s10895-022-02923-4

[24] Licht, F., Davis, M.A., Andreas, H.A. (2020). Charge redistribution and electrode history impact galvanostatic charging/discharging and associated figures of merit. Journal of Power Sources, 446: 227354. https://doi.org/10.1016/j.jpowsour.2019.227354

[25] Yang, X., Wan, Y., Zheng, Y., He, F., Yu, Z., Huang, J., Wang, H., Ok, Y.S., Jiang, Y., Gao, B. (2019). Surface functional groups of carbon-based adsorbents and their roles in the removal of heavy metals from aqueous solutions: A critical review. Chemical Engineering Journal, 366: 608-621. https://doi.org/10.1016/j.cej.2019.02.119

[26] Kim, S., Kim, J., Kim, M., Cho, M., Lee, Y. (2021). Aqua-Processable carbon quantum dot-Assisted resilient polymer binder for advanced lithium-sulfur batteries. International Journal of Energy Research, 45(15): 21050-21057. https://doi.org/10.1002/er.7162

[27] El-Shamy, A.G. (2019). Novel conducting PVA/Carbon quantum dots (CQDs) nanocomposite for high anti-electromagnetic wave performance. Journal of Alloys and Compounds, 810: 151940. https://doi.org/10.1016/j.jallcom.2019.151940

[28] Lazanas, A.C., Prodromidis, M.I. (2023). Electrochemical impedance spectroscopy-A tutorial. ACS Measurement Science Au, 3(3): 162-193. https://doi.org/10.1021/acsmeasuresciau.2c00070

[29] Sihombing, Y.A., Rahayu, S.U., Situmeang, M.D. (2023). Effect of reduced graphene oxide (rGO) in chitosan/Pahae natural zeolite-based polymer electrolyte membranes for direct methanol fuel cell (DMFC) applications. Materials Science for Energy Technologies, 6: 252-259. https://doi.org/10.1016/j.mset.2023.01.002

[30] Ridwan, F., Febriyan, N., Husin, M.A., Aulia, F. (2024). Developing sustainable reinforcement PLA/NCC from kapok to improve mechanical and electrical properties composites with PVA Matrix. Journal of Composite & Advanced Materials/Revue des Composites et des Matériaux Avancés, 34(5): 613-619. https://doi.org/10.18280/rcma.340509